Seismic reliability analysis of isolated deck bridges using friction pendulum devices

Available online at www.sciencedirect.com

ScienceDirect

Procedia Structural Integrity 44 (2023) 1435–1442

Structural Integrity Procedia

www.elsevier.com/locate/procedia

XIX ANIDIS Conference, Seismic Engineering in Italy

Seismic reliability analysis of isolated deck bridges using friction pendulum devices

Diego Gino[a], Elena Miceli[a], Paolo Castaldo[a]*

[a]*Department of Structural, Geotechnical and Building Engineering (DISEG), Politecnico di Torino, 10129, Turin, Italy*

Abstract

In this study, the seismic reliability of multi-span continuous deck bridges equipped with isolation friction pendulum (FP) devices is investigated. The relevant aleatory uncertainties associated to the sliding friction coefficient of the FP isolators and to the seismic inputs are considered. A six-degree-of-freedom model is established to reproduce the elastic behavior of the reinforced concrete (RC) pier, the stiff response of the deck supported by the isolation devices and the non-linear response of the FPS bearings which depends on the sliding velocity. Moreover, the RC abutment is assumed as infinitely rigid. For what concerns the seismic inputs, a group of natural seismic records having various characteristics is adopted and properly scaled to increasing levels of intensity. The random variability of the friction coefficient is modelled by suitable probabilistic distribution. Then, considering several bridges and isolator configurations, the fragility curves of the RC pier and of the isolator devices (FP) are determined. Finally, in agreement with the hazard curve of the specific site, the convolution integral is adopted to determine the seismic reliability curves in the performance domain.

Keywords: seismic assessment; bridges; friction pendulum system; performance-based design; structural reliability.

1. Introduction

The adoption of passive control (e.g., isolation) is, nowadays, one of the most efficient solution to increase the seismic protections of buildings and infrastructures (Nastri et al. (2000), Troisi and Alfano (2022a,b,c), Troisi and Arena (2022), Troisi and Castaldo (2022), Troisi et al. (2021)). Concerning the case of bridges, their safety assessment is one of the main topics for engineers and Authorities (Gino et al., (2020), Castaldo et. Al (2021), Gino et al. (2021)). In particular, the isolation technique permits to uncouple the response of the deck from the seismic motion in horizontal

* Corresponding author. Tel.: +39-011-090-5307.
E-mail address: paolo.castaldo@polito.it

2452-3216
10.1016/j.prostr.2023.01.184

direction. By this way, the acceleration of the deck and the related forces transmitted to the pier are significantly reduced with respect to bridges which are not isolated (Jangid (2008), Castaldo et al. (2018a), Castaldo et al. (2020)). In this framework, Castaldo and Alfano (2020) have introduced the seismic reliability-based design (SRBD) approach to provide tools useful to design isolation devices including the relevant sources of uncertainties. The present analysis deals with the seismic reliability of multi-span continuous deck bridges equipped with friction pendulum system (FPS). In particular, the principal aleatoric uncertainties associated to the sliding friction coefficient of the FPS isolators and to the seismic inputs are considered. A six-degree-of-freedom model is defined to simulate the elastic response of the reinforced concrete (RC) pier, the response of the deck (assumed as stiff) located on the FPS seismic devices and the non-linear behaviour of the FPS bearings which depends on the sliding velocity (Castaldo and Ripani (2017), Auad et al. (2022)). The RC abutment is modelled as a rigid support above which a FPS device is placed (Wang et al. (1998), Kunde and Jangid (2003)). The FPS device behaviour has been modelled as suggested by (Mokha (1990)). Adopting the friction coefficient as the main random variable, it has been modelled by means of normal distribution and the Latin hypercube Sampling Method (LHS) has been used (Celarec and Dolsek (2013)) to perform probabilistic analysis. Furthermore, a set of 30 natural seismic records having various spectral characteristics has been collected to consider the uncertainty in the seismic action. The considered spectra are scaled to growing levels of intensity in relation to the seismic hazard of the L'Aquila (Italy) site. Then, incremental dynamic analyses (IDAs) (Vamvatsikos and Cornell (2002)) have been performed to characterize the seismic demand and the capacity of the specific bridge. The estimates of the response parameters (i.e., peak deck displacement with respect to the pier and to the abutment and peak pier displacement with respect to the ground) have been adopted to assess the seismic fragility curves (Montuori et al. (2019)) of the isolators (and of the deck) and of the RC pier. The mentioned above fragility curves can be adopted to evaluate the seismic reliability of the bridge equipped with FPS in line to Cornell and Krawinkler (2000) adopting the site-specific hazard curves and the appropriate reference period.

Nomenclature

u_d	displacement in horizontal direction of the deck relative to the pier
u_{pi}	displacement of the i^{th} (i:1-5) lumped mass of the pier with respect to the i^{th}-1 dof
m_d	mass of the deck
m_{pi}	mass of tht i^{th} (i:1-5) lumped mass of the pier
c_d	constant value of viscous damping of the deck
k_{pi}	stiffness related of the i^{th} (i:1-5) dof of the pier
c_{pi}	constant viscous damping related of the i^{th} (i:1-5) dof of the pier
t	time
$f_p(t)$	reactions of the FP isolators on the pier
$f_a(t)$	reactions of the FP isolators on the abutment
g	acceleration of gravity
R	FPS radius of curvature
r	in plane radius of the FPS
μ	friction coefficient of the FP device
S_D	spectral displacement related to the isolated fundamental period of the bridge
T_d	isolated fundamental period of the bridge
ξ_d	damping ratio of the bridge the deck with isolation
ξ_{pi}	damping ratio of the i^{th} lumped mass of the pier
ω_d	circular frequency of the deck with isolation
ω_{pi}	circular frequency of the i^{th} dof of the pier
λ_{pi}	mass ratio of the i^{th} dof of the pier
f_{max}	sliding friction coefficient at high velocity
f_{min}	sliding friction coefficient at low velocity

2. Response of bridges isolated with FPS

In line to Jangid (2008), Kunde and Jangid (2009), the structural behaviour of an isolated three-span continuous deck bridge (Figure 1), is reproduced in this work adopting the following modelling strategy: 5 dof relates to the lumped masses of the RC pier and 1 dof to the mass of the stiff RC deck. As introduced before, the RC abutment is considered as infinitely rigid. The dynamic equilibrium equations which control the behaviour of a bridge isolated with FPS subjected to seismic action according to configuration of Figure 1 described by the expressions of Eq.(1).

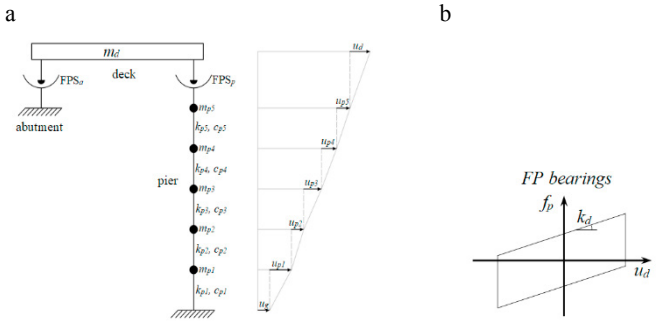

Fig. 1. (a) Modelling of the bridge of FPS devices by means of 6 dof model; (b) force-displacement response of the FPS on the RC pier.

$$
\begin{aligned}
&m_d\ddot{u}_d(t)+m_d\ddot{u}_{p5}(t)+m_d\ddot{u}_{p4}(t)+m_d\ddot{u}_{p3}(t)+m_d\ddot{u}_{p2}(t)+m_d\ddot{u}_{p1}(t)+c_d\dot{u}_d(t)+f_b(t)+f_a(t)=-m_d\ddot{u}_g(t)\\
&m_{p5}\ddot{u}_{p5}(t)+m_{p5}\ddot{u}_{p4}(t)+m_{p5}\ddot{u}_{p3}(t)+m_{p5}\ddot{u}_{p2}(t)+m_{p5}\ddot{u}_{p1}(t)-c_d\dot{u}_d(t)+c_{p5}\dot{u}_{p5}(t)+k_{p5}u_{p5}(t)-f_b(t)=-m_{p5}\ddot{u}_g(t)\\
&m_{p4}\ddot{u}_{p4}(t)+m_{p4}\ddot{u}_{p3}(t)+m_{p4}\ddot{u}_{p2}(t)+m_{p4}\ddot{u}_{p1}(t)-c_{p5}\dot{u}_{p5}(t)-k_{p5}u_{p5}(t)+c_{p4}\dot{u}_{p4}(t)+k_{p4}u_{p4}(t)=-m_{p4}\ddot{u}_g(t)\\
&m_{p3}\ddot{u}_{p3}(t)+m_{p3}\ddot{u}_{p2}(t)+m_{p3}\ddot{u}_{p1}(t)-c_{p4}\dot{u}_{p4}(t)-k_{p4}u_{p4}(t)+c_{p3}\dot{u}_{p3}(t)+k_{p3}u_{p3}(t)=-m_{p3}\ddot{u}_g(t)\\
&m_{p2}\ddot{u}_{p2}(t)+m_{p2}\ddot{u}_{p1}(t)-c_{p3}\dot{u}_{p3}(t)-k_{p3}u_{p3}(t)+c_{p2}\dot{u}_{p2}(t)+k_{p2}u_{p2}(t)=-m_{p2}\ddot{u}_g(t)\\
&m_{p1}\ddot{u}_{p1}(t)-c_{p2}\dot{u}_{p2}(t)-k_{p2}u_{p2}(t)+c_{p1}\dot{u}_{p1}(t)+k_{p1}u_{p1}(t)=-m_{p1}\ddot{u}_g(t)
\end{aligned}
\tag{1}
$$

The term u_d represents the displacement in horizontal direction of the deck relative to the pier, u_{pi} is the displacement of the i^{th} (i:1-5) lumped mass of the pier with respect to the i^{th}-1 dof, m_d and m_{pi} respectively the mass of the deck and of the i^{th} (i:1-5) lumped mass of the pier, c_d is the constant value of viscous damping of the deck, k_{pi} and c_{pi} are the stiffness of the pier and related viscous damping constant of the i^{th} (i:1-5) dof, t is the time, $f_p(t)$ and $f_a(t)$ are the reactions of the FP isolators on the pier and on the abutment evaluated as:

$$
f_p(t)=\frac{m_d g u_d(t)}{2R}+\frac{\mu_p(\dot{u}_d)m_d g\,\mathrm{sgn}(\dot{u}_d)}{2} \tag{2a}
$$

$$
f_a(t)=\frac{m_d g}{2R}\left(u_d(t)+\sum_{i=1}^{5}u_{pi}\right)+\frac{1}{2}\left(\mu_a\left(\dot{u}_d(t)+\sum_{i=1}^{5}\dot{u}_{pi}\right)\right)m_d g\left(\mathrm{sgn}\left(\dot{u}_d(t)+\sum_{i=1}^{5}\dot{u}_{pi}\right)\right) \tag{2b}
$$

where g is the acceleration of gravity, R denotes the FPS radius of curvature, $\mu(\dot{u}(t))$ is the friction coefficient of the FP device on the abutment (a) or of the isolator on the pier (p), which depends on the sliding velocity and, finally, sgn(·) is the sign function. The variation of $\mu(\dot{u}(t))$ can be reproduced according to the results of Mokha et al. (1990) and Constantinou et al. (1990) as also performed by Castaldo and Ripani (2017). By means the division of the Eq.(1)-(2) by the value of the deck mass m_d, the related dimensionless equations can be evaluated according to following parameters: mass ratio of the i^{th} dof of the pier $\lambda_{pi}=m_{pi}/m_d$; damping ratio of the deck with isolation and of

the i[th] lumped mass of the pier, respectively $\xi_d = \frac{c_d}{2m_d\omega_d}$, $\xi_{pi} = \frac{c_{pi}}{2m_{pi}\omega_{pi}}$; circular frequency of the deck with isolation and of the i[th] dof of the pier , repectively, $\omega_d = \frac{2\pi}{T_d} = \sqrt{\frac{g}{R}}$, $\omega_{pi} = \sqrt{\frac{k_{pi}}{m_{pi}}}$.

3. Uncertainties within seismic reliability analysis

In line with the performance-based earthquake engineering (PBEE) approach Cornell and Krawinkler (2000), the present investigation accounts for separately the uncertainties associated to the intensity of seismic event from the ones referred to characteristics of the specific record. With this approach, the random variability of the intensity of seismic event can be represented by means a hazard curve. In this circumstance, the randomness of ground motion (associated to fixed intensity level) can be described by a set records having variable duration and content in terms of frequency by scaling these records to common value of intensity measure (IM). In particular, 30 natural records, descending from 19 earthquake events, have been adopted in line to Castaldo and Amendola (2021) considering the horizontal component only. The list of records reported by Table A1 in the Appendix. The spectral-displacement S_D (T_d, ξ_d), related to the isolated fundamental period of the bridge $T_d=2\pi/\omega_d$ and for the damping ratio ξ_d, has been adopted as IM. According to Castaldo et al. (2018b), ξ_d can be set reasonably equal to zero. Then, the value $S_D(T_d)$ is assumed ranging from 0.10m to 0.45m to perform the IDAs. A further random variable has been included in probabilistic analysis: the friction coefficient on sliding surface. In particular, a normal distribution truncated between 0.5% to 5.5%, with mean value set equal to 3%, has been used to probabilistically model the sliding friction coefficient at high velocity f_{max} (Castaldo and Alfano (2020)). With reference to the model of Constantinou et al. (1990), the values of the friction coefficient at the low velocities, f_{min} have been considered dependent random variable and set equal to $f_{max}/3$. The Latin Hypercube (LH) sampling method Castaldo and Amendola (2021) has been adopted to generate the samples to define the structural numerical models. A total number of 15 samples has been defined from the mentioned above PDF. The study is organized by large parametric analysis which involves different characteristics associated to bridges with isolation devices. In particular, the parameters ξ_d and $\xi_{pi}= \xi_p$ are adopted as deterministic and set respectively equal to 0% and 5%; the isolated super-structure period T_d ranges between 1s, 2s, 3s and 4s; the RC pier period T_p varies between 0.05s, 0.01s, 0.15s and 0.2s and is associated to the five vibration modes of the dof considered to model the pier; λ, which denotes the overall mass ratio related to the sum of the i[th] mass ratios, ranges between 0.1, 0.15 and 0.2. The field of variation of the mentioned above parameters is in agreement to Castaldo et al. (2018b). With this approach, the combination of the selected parameters leads to the definition of 720 different types of bridges equipped with isolators.

4. Outcomes from IDA investigation

Concerning each one of the 720 combinations between the parameters assumed in the parametric study, the differential equations of Eq (1) have been solved considering the 30 seismic records (Table A1), which are scaled to increasing values of $S_D(T_d)$. For each bridge configuration, a total number of 450 simulations have been performed coupling the 15 sampled values of the friction coefficient to the 30 seismic records scaled at the specific IM.

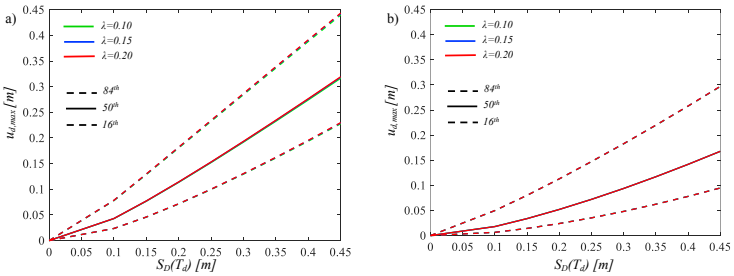

Fig. 2. IDAs related to the deck displacement referred to the pier. (T_p=0.05s and T_d =1s (a), T_d =4s (b)).

The IDAs have been determined adopting the following engineering demand parameters (EDPs): the top pier

displacement u_p referred to the ground (determined as the sum of u_{pi} *i:1-5*), the deck displacement referred, respectively, to the top of the pier u_d and to the abutment $u_{d,abut}$ (determined as the sum of u_d and u_p). For all the engineering demand parameters, the peak values are assessed and then a set of samples is obtained for each EDP at each value of the *IM*. The output set has been probabilistically treated by means of a lognormal distribution. The sample of data, which characterize the structural responses, represents the demand in terms of displacement for both the deck and the pier. With reference to the single EDP, a lognormal distribution can be determined evaluating the statistical parameters using the maximum likelihood technique Castaldo and Amendola (2021). Then, is possible to estimate the 50th, 84th, 16th percentiles of each considered probabilistic distribution Castaldo and Amendola (2021). The results of the IDA related to the deck (i.e., of the seismic device located on the pier and on the abutment) as well as the IDA curves of the pier can be determined as reported in **Errore. L'origine riferimento non è stata trovata.** and 3. After the determination of the EDPs from the IDAs it is possible to estimate the probabilities P_f exceeding different limit states (LSs) conditional to specific level of the IM as previously introduced. With reference to the LS thresholds associated to the FP isolator devices, nine values of the in plane radius of the single concave surface have been considered with the range 0.10-0.5m (Castaldo and Ripani (2017)). Concerning the thresholds related to the RC pier, four performance levels (LS1, LS2, LS3 and LS4), related to "fully operational", "operational", "life safety" and "collapse prevention", are established by SEAOC Vision 2000. In line to the displacement-based seismic design, the measurable structural response parameter, pier drift index (PDI), is adopted to define the specific LS threshold the reference life of a structural system. The PDI is defined as the ratio between the maximum to displacement of the pier and the height of the pier.

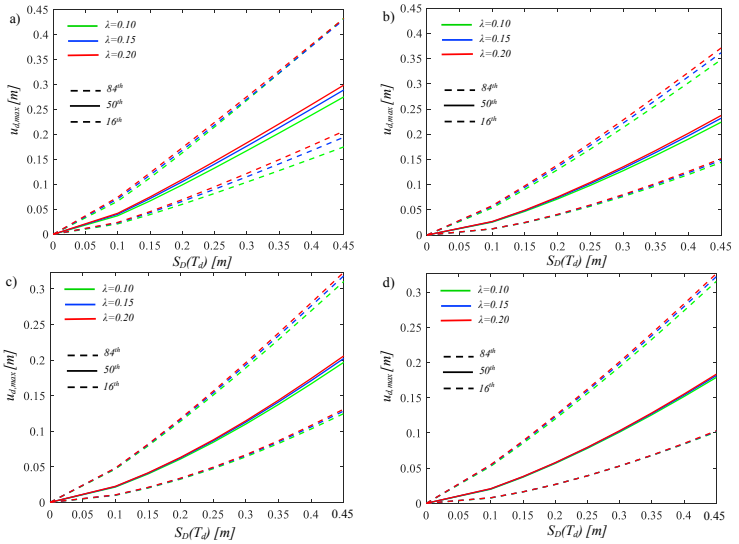

Fig. 3. IDAs related to the deck displacement referred to the pier. (T_p=0.20s and T_d =1s (a), T_d =2s (b), T_d =3s (c), T_d =4s (d)).

5. Seismic reliability analysis

The mean annual rates of exceedance for the LSs can be derived performing convolution integral between the seismic fragility and seismic hazard curves Castaldo and Alfano (2020).

In this investigation, the site of L'Aquila (Italy) is considered and the associated hazard curves for seismic action are reported in Figure 4.

The mean annual rate and related probability (concerning 50 years as reference life) of exceeding the corresponding LS for isolation devices and the pier, can be determined as:

$$\lambda_{LS} = \int P_f(IM) \cdot \left| \frac{d\bar{\lambda}_{IM}(IM)}{d(IM)} \right| d(IM) \tag{3}$$

$$P_f(50 years) = 1 - e^{\lambda_{LS} \cdot (50 years)} \tag{4}$$

Figures 5, 6 and 7 show the seismic reliability curves for the RC pier and for the deck responses. In Figures 6 and 7, *r* is the in plane radius of the FPS device expressed in meters.

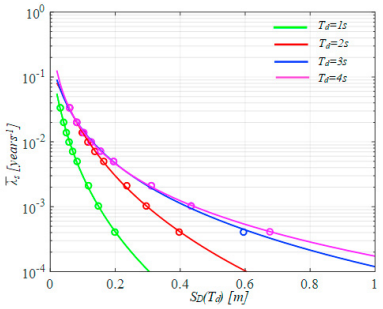

Fig. 4. Average annual rates of exceedance of the IM $S_D(T_d)$ – hazard curves . (L'Aquila site).

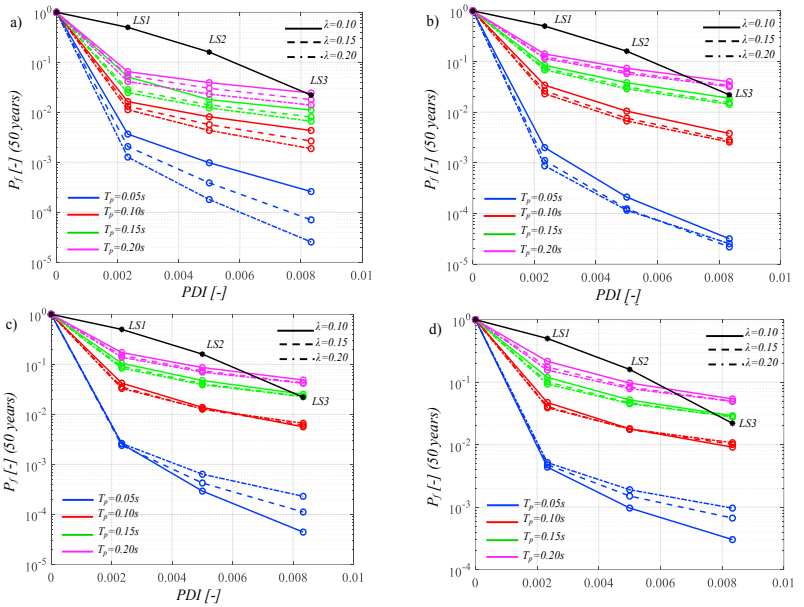

Fig. 5. Representation of the seismic reliability curves associated to the pier for T_d =1s (a), T_d =2s (b), T_d =3s (c), T_d =4s.

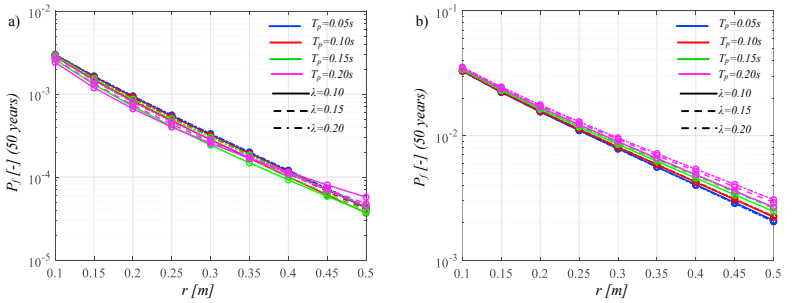

Fig. 6. Representation of the seismic reliability curves associated to the deck response referred to the pier for T_d =1s (a), T_d =4s (b).

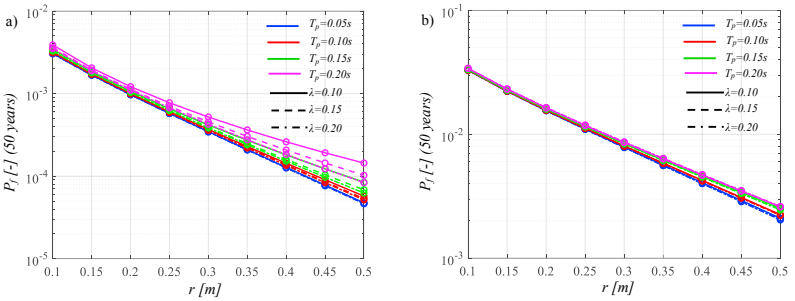

Fig. 7. Representation of the seismic reliability curves associated to the deck response referred to the abutment for Td =1s (a), Td =4s (b).

6. Conclusions

This study relates to the seismic reliability of multi-span continuous deck bridges equipped with single concave friction pendulum (FPS) devices. A wide parametric study has been carried out taking into account several bridge configurations (i.e., differentiating the vibration period of the RC pier in elastic field, the isolating system period and the ratio between the pier and the deck mass). The seismic reliability assessment leads to the following results:

i. With reference to the pier, the fully operational and operational limit states are fulfilled in all situations demonstrating the effectiveness of the seismic isolation devices.
ii. Concerning the isolator devices (i.e., of the deck) the seismic reliability decreases with the increase of the radius of curvature of the FP device due to the high seismic hazard of the considered site.

With reference to assessment/design of multi-span continuous deck bridges located in areas with significant seismic hazard, the achieved results are helpful to define rules for the preliminary design of the isolation system in line to target reliability levels associated to the related reference life.

Appendix A.

Summary of the seismic records adopted for reliability analysis:

	Year	Earthquake	Recording Station	Vs_{30} [m/sec]	Fault type	M [-]	R [km]	PGA_m [g]
1	1994	Northridge	Beverly Hills - Mulhol	356	Thrust	6.7	13.3	0.52
2	1994	Northridge	Canyon Country-WLC	309	Thrust	6.7	26.5	0.48
3	1994	Northridge	LA – Hollywood Stor	316	Thrust	6.7	22.9	0.36
4	1999	Duzce, Turkey	Bolu	326	Strike-slip	7.1	41.3	0.82
5	1999	Hector Mine	Hector	685	Strike-slip	7.1	26.5	0.34
6	1979	Imperial Valley	Delta	275	Strike-slip	6.5	33.7	0.35
7	1979	Imperial Valley	El Centro Array #11	196	Strike-slip	6.5	29.4	0.38
8	1995	Kobe, Japan	Nishi-Akashi	609	Strike-slip	6.9	8.7	0.51
9	1995	Kobe, Japan	Shin-Osaka	256	Strike-slip	6.9	46	0.24
10	1999	Kocaeli, Turkey	Duzce	276	Strike-slip	7.5	98.2	0.36
11	1999	Kocaeli, Turkey	Arcelik	523	Strike-slip	7.5	53.7	0.22
12	1992	Landers	Yermo Fire Station	354	Strike-slip	7.3	86	0.24
13	1992	Landers	Coolwater	271	Strike-slip	7.3	82.1	0.42
14	1989	Loma Prieta	Capitola	289	Strike-slip	6.9	9.8	0.53
15	1989	Loma Prieta	Gilroy Array #3	350	Strike-slip	6.9	31.4	0.56
16	1990	Manjil, Iran	Abbar	724	Strike-slip	7.4	40.4	0.51
17	1987	Superstition Hills	El Centro Imp. Co.	192	Strike-slip	6.5	35.8	0.36
18	1987	Superstition Hills	Poe Road (temp)	208	Strike-slip	6.5	11.2	0.45
19	1987	Superstition Hills	Westmorland Fire Stat.	194	Strike-slip	6.5	15.1	0.21
20	1992	Cape Mendocino	Rio Dell Overpass	312	Thrust	7.0	22.7	0.55
21	1999	Chi-Chi, Taiwan	CHY101	259	Thrust	7.6	32	0.44
22	1999	Chi-Chi, Taiwan	TCU045	705	Thrust	7.6	77.5	0.51
23	1971	San Fernando	LA - Hollywood Stor	316	Thrust	6.6	39.5	0.21
24	1976	Friuli, Italy	Tolmezzo	425	Thrust	6.5	20.2	0.35
25	1980	Irpinia	Bisaccia	496	-	6.9	21.3	0.94
26	1979	Montenegro	ST64	1083	Thrust	6.9	21.0	0.18

27	1997	Umbria Marche	ST238	n/a	Normal	6.0	21.5	0.19
28	2000	South Iceland	ST2487	n/a	Strike-slip	6.5	13	0.16
29	2000	South Iceland (a.s.)	ST2557	n/a	Strike-slip	6.5	15.0	0.13
30	2003	Bingol	ST539	806	Strike-slip	6.3	14.0	0.30

Source: PEER, ITACA, ISESD-Internet Site for European Strong-Motion Data

References

Auad G., Castaldo P., Almazán J.L., 2022. Seismic reliability of structures equipped with LIR-DCFP bearings in terms of superstructure ductility and isolator displacement. Earthquake Engineering and Structural Dynamics,10.1002/eqe.3719.

Castaldo P., Alfano G., 2020. Seismic reliability-based design of hardening and softening structures isolated by double concave sliding devices. Soil Dynamics and Earthquake Engineering, 129, 105930.

Castaldo P., Amendola G., 2021. Optimal DCFP bearing properties and seismic performance assessment in nondimensional form for isolated bridges. Earthquake Engineering and Structural Dynamics, https://doi.org/10.1002/eqe.3454.

Castaldo, P., Amendola, G., Gino, D. Miceli, E., 2020. Seismic performance of bridges isolated with DCFP devices. Proceedings of the International Conference on Structural Dynamic, EURODYN, 1704-1721.

Castaldo P., Gino D., Marano G.C., Mancini G. 2022. Aleatory uncertainties with global resistance safety factors for non-linear analyses of slender reinforced concrete columns, Engineering Structures, 255, 113920

Castaldo P., Palazzo B., Alfano G., Palumbo M.F., 2018a. Seismic reliability-based ductility demand for hardening and softening structures isolated by friction pendulum bearings. Structural Control and Health Monitoring, 25(11), e2256, https://doi.org/10.1002/stc.2256.

Castaldo P., Ripani M., 2017. Optimal design of single concave sliding bearings for isolated structures considering intermediate isolation degrees. Ingegneria Sismica, 34(3-4), 5–23.

Castaldo P., Ripani M., 2017. Optimal design of single concave sliding bearings for isolated structures considering intermediate isolation degrees. Ingegneria Sismica, 34(3-4), 5–23.

Castaldo P., Ripani M., Lo Piore R., 2018b. Influence of soil conditions on the optimal sliding friction coefficient for isolated bridges. Soil Dynamics and Earthquake Engineering, 111, 131–148, 2018b https://doi.org/10.1016/j.soildyn.2018.04.056.

Celarec D., Dolšek M., 2013. The impact of modelling uncertainties on the seismic performance assessment of reinforced concrete frame buildings. Engineering Structures, 52, 340-354.

Constantinou M.C., Mokha A., Reinhorn A.M., 1990. Teflon Bearings in Base Isolation. II: Modeling. Journal of Structural Engineering, 116(2), 455-474.

Cornell C.A., Krawinkler H., 2000. Progress and challenges in seismic performance assessment. PEER Center News, 4(1), 1-3.

Gino D., Castaldo P., Bertagnoli G., Giordano L., Mancini G., 2020. Partial factor methods for existing structures according to fib Bulletin 80: Assessment of an existing prestressed concrete bridge. Structural Concrete; 21, 15-31, 2020 https://doi.org/10.1002/suco.201900231.

Gino D., Castaldo P., Giordano, L. Mancini, G. 2021. Model uncertainty in non-linear numerical analyses of slender reinforced concrete members. Structural Concrete, 22(2), pp. 845–870

Jangid R.S., 2008. Stochastic response of bridges seismically isolated by Friction Pendulum System. Journal of Bridge Engineering, 13(4), 319-330.

Kunde M.C., Jangid R.S., 2003. Seismic behavior of isolated bridges: A-state-of-the-art review. Electronic Journal of Structural Engineering, 3.

Mokha A., Constantinou M.C., Reinhorn A.M., 1990. Teflon Bearings in Base Isolation. I: Testing. Journal of Structural Engineering, 116(2), 438-454.

Montuori R., Nastri E., Piluso V., 2019. Problems of modeling for the analysis of the seismic vulnerability of existing buildings. Ingegneria Sismica, 36(2), 53-85.

Nastri E., D'Aniello M., Zimbru M., Streppone S., Landolfo, R., Montuori R.,Piluso, V., 2000. Seismic response of steel Moment Resisting Frames equipped with friction beam-to-column joints. Soil Dynamics and Earthquake Engineering, 119, 144-157.

Porter K.A., 2003. An overview of PEER's performance-based earthquake engineering methodology. Proceedings of the 9th International Conference on Application of Statistics and Probability in Civil Engineering (ICASP9), San Francisco, California.

SEAOC Vision 2000 Committee, 2005. Performance-based seismic design engineering. Report prepared by Structural Engineers Association of California, Sacramento, CA

Troisi, R., Alfano, G. 2022a. Is regional emergency management key to containing COVID-19? A comparison between the regional Italian models of Emilia-Romagna and Veneto. International Journal of Public Sector Management, 35(2), 195–210. DOI: 10.1108/IJPSM-06-2021-0138.

Troisi R., Alfano G. 2022. The re-election of corrupt mayors: context, relational leadership and level of corruption. Local Government Studies. https://doi.org/10.1080/03003930.2022.2087060.

Troisi R., Alfano G. 2022c. Proximity and inter-firm corruption: A transaction cost approach, Small Business Economics. DOI10.1007/s11187-022-00649-y.

Troisi, R., Arena, L. 2022. Organizational Aspects of Sustainable Infrastructure Safety Planning by Means of Alert Maps. Sustainability (Switzerland) 14(4), 2335.

Troisi R., Castaldo P., 2022. Technical and organizational challenges in the risk management of road infrastructures, Journal of Risk Research, 25(6), 791-806, DOI:10.1080/13669877.2022.2028884.

Troisi R., Di Nauta P., Piciocchi P. 2021. Private corruption: An integrated organizational model. European Management Review. https://doi.org/10.1111/emre.12489.

Vamvatsikos D., Cornell C.A., 2002. Incremental dynamic analysis. Earthquake Engineering and Structural Dynamics, 31(3), 491–514.

Wang Y. P., Chung L. L.., Liao W. H., 1998. Seismic response analysis of bridges isolated with friction pendulum bearings. Earth. Eng. & Str. Dyn., 27, 1069-1093.